Supplementary Information

SI Materials and Methods

Protein purification

E. coli BL21(DE3) transformed with the pET28a_PPHD or pET28a_EF-Tu plasmid (encoding for proteins with an *N*-terminal hexahistidine tag) were grown (37 °C; 180 rpm) to an OD_{600} of 0.6; recombinant protein expression was induced with 0.5 mM β-D-1-thiogalactopyranoside (IPTG). The cells were then grown at 18°C overnight, harvested by centrifugation (10,000x*g*; 7 min), and stored at -80 °C. Cell pellets (for PPHD:EF-Tu complex, 1:1 w/w) were resuspended in 50 mM HEPES pH 7.5, 500 mM NaCl, 20 mM imidazole, 1 mM tris(2-carboxyethyl)phosphine (TCEP), one EDTA-free protease inhibitor tablet (Roche), and approximately 1 mg DNAseI (bovine pancreas, grade II, Roche) at room temperature with gentle stirring. Cells were lysed on ice by sonication and the lysate was cleared by centrifugation (50,000x*g*; 20 min). The supernatant was then loaded onto a 5 mL HisTrap FF column preequilibrated with the resuspension buffer and purified using an AKTA FPLC system (GE Healthcare). The column was washed with 10 column volumes of 50 mM HEPES pH 7.5, 500 mM NaCl, 50 mM imidazole, 1 mM TCEP and protein was eluted with 50 mM HEPES pH 7.5, 500 mM NaCl, 250 mM imidazole, 1 mM TCEP. The purified sample was then exchanged to 50 mM HEPES pH 7.5, 200 mM NaCl using a PD-10 column (Millipore). PPHD, EF-Tu, or the PPHD:EF-Tu protein-protein complex were further purified using a Superdex 75 size exclusion column (GE Healthcare) preequilibrated in 50 mM HEPES pH 7.5, 200 mM NaCl (PPHD), 50 mM HEPES pH 7.5, 200 mM NaCl, 10 mM $MgCl_2$, 1 μM GDP (EF-Tu), or 50 mM HEPES pH 7.5, 10 mM $MgCl_2$, 1 μM GDP (PPHD:EF-Tu complex). Proteins were eluted using the same buffer. PPHD-, EF-Tu-, or PPHD:EF-Tu-containing fractions were pooled, concentrated to 35 mg/mL (PPHD), 20 mg/mL (EF-Tu), or 15 mg/mL (PPHD:EF-Tu) by diafiltration, aliquoted (20 μL), flash frozen in liquid N_2, and stored at -80 °C.

X-ray crystallography

Crystals of PPHD in complex with NOG and crystals of PPHD:EF-Tu complex were grown in sitting drops using the vapor diffusion method (drop size: 200-300 nL) at 293 K in 96-well Intelliplates (Art Robbins); crystals of EF-Tu were grown at 277 K. Crystals were cryo-protected by transfer to 25% (v/v) glycerol in well solution and then harvested in nylon loops (Hampton Research) and cryo-cooled by plunging in liquid nitrogen. Data were collected at 100 K using single crystals at Diamond Light Source beamline I04 (PPHD:Mn(II):NOG and PPHD:EF-Tu complex) with a ADSC Quantum 315r detector, and Diamond Light Source beamline I03 (EF-Tu:Mg(II):GDP) with a Pilatus 6M-F detector. Data were then indexed, integrated, and scaled using SCALA (PPHD:Mn(II):NOG)(1), HKL3000 (EF-Tu:Mg(II):GDP)(2), and XSCALE (PPHD:EF-Tu complex)(3, 4). The structure of PPHD:Mn(II):NOG was determined by molecular replacement (MR) using the MR-PHASER (5) subroutine of PHENIX (6) using *H. sapiens* PHD2 (PDB ID: 2G1M) as the search model. The EF-Tu:Mg(II):GDP was determined by MR using *E. coli* EF-Tu (PDB ID: 1DG1) as the search model. The PPHD:EF-Tu protein-protein complex was determined by MR using *E. coli* EF-Tu (PDB ID: 1DG1) and the refined PPHD:Mn(II):NOG as search models. Model building and refinement were performed iteratively using COOT (7) and PHENIX until converging *R* and *R*free no longer decreased. Mn(II), Mg(II), NOG, and GDP and water molecules were modelled in the final stages of refinement based on the $F_{obs} - F_{calc}$ electron density map.

A *PPHD* (*PA0310*) deleted strain of *P. aeruginosa*

A *Pseudomonas aeruginosa* PAO1 strain containing a Tn5 transposon insert in the *PA0310* gene was obtained from the PAO1 mutant library generated and verified by the University of Washington Genome Sciences as described (8).

***P. aeruginosa* growth determination**

Immediately upon dilution, cultures in triplicate, in 96-well plates, were placed in a plate reader (Infinite M200; TECAN) at 28 °C and grown within the plate reader. The optical density at 600 nm (OD_{600}) was automatically read during growth every 60 min, and data were collected by Magelan software (TECAN). All assays were performed in triplicate and plotted as mean ± standard deviation.

***P. aeruginosa* pyocyanin quantification**

Cultures (5 mL) of *P. aeruginosa* wildtype and *PA0310* deletion strains grown to stationary phase were extracted with 3 mL of $CHCl_3$ and back extracted with 1 mL of 0.2 HCl, yielding a deep red solution, of which the aqueous phase was decanted and the absorbance was measured at 520 nm as reported previously (9). All assays were performed in triplicate and plotted as mean ± standard deviation.

***P. aeruginosa* global translation rate assay**

Cultures (1 mL) of *P. aeruginosa* wildtype and *PA0310* deletion strains were grown in LB medium at 37 °C with shaking to log phase (OD_{600} = 0.5), whereupon ^{35}S-methionine was added to a final concentration of 10 µCi/mL and growth was continued at 37 °C with shaking. At the specified timepoints 100 µl was removed from biological triplicates and placed on ice before the addition of 10 µl BSA (4 mg/mL) and 20 µl 50% (w/v) trichloroacetic acid (Sigma). The protein pellet was isolated by centrifugation (25,000x*g*; 2 min), washed twice with 300 µl of cold ethanol, and solubilized in 50 µl 8 M urea. 10 µl was then added to 5 mL of Optiphase scintillant and ^{35}S-methionine incorporation was measured by scintillation counting.

PPHD pull-down in *P. putida*

Pseudomonas putida substrain KT2440 was grown (37 °C; 180 rpm) overnight in LB media, harvested by centrifugation (10,000x*g*; 7 min), resuspended in binding buffer (50 mM Tris-HCl pH 7.5, 125 mM NaCl, 5 mM imidazole) lysed on ice by sonication and the lysate was cleared by centrifugation (50,000x*g*; 20 min). 1 mL of cleared lysate was added to loose Ni-Sepharose beads (GE Healthcare), preincubated for 1 hour with 1 mg of pure hexahistidine-tagged PPHD in binding buffer, and washed three times with the same buffer. Proteins were eluted from the beads in elution buffer (50 mM Tris-HCl pH 7.5, 500 mM NaCl, 250 mM imidazole), precipitated in MeOH/$CHCl_3$, then subjected to trypsinolysis and MS/MS quantitation and analysis using Mascot as described (10).

PPHD kinetic assays

Standard hydroxylation assays for $PPHD_{putida}$ were carried out by preparing a reaction mixture of 10 µM PPHD, 100 µM EF-$Tu_{44\text{-}63}$ (H_2N-IVEFDKIDSAPEEKARGITI-$CONH_2$), 50 µM Fe(II)(prepared from $(NH_4)_2Fe(SO_4)_2$), 2 mM 2OG, 4 mM sodium L-ascorbate in 50 mM HEPES pH 7.5, 500 mM NaCl, 5% (v/v) glycerol with a final volume of 20 µL. For determinations of apparent K_m of Fe(II), 2OG, ascorbate, and O_2, each cofactor concentration was varied and reactions were incubated at 37 °C for 30 minutes. For determination of apparent K_m of EF-$Tu_{44\text{-}63}$ oligopeptide time courses at various concentrations of EF-$Tu_{44\text{-}63}$ were carried out and steady-state reaction rates were determined. All reactions were quenched with 1:1 (v/v) 20% (v/v) formic acid. The extent of substrate hydroxylation was analyzed by MALDI-TOF-MS (matrix-assisted laser-desorption ionization–time-of-flight mass spectrometry). Recrystallized CHCA (α-cyano-4-hydroxycinnamic acid) MALDI matrix (1 µL) and quenched assay solution (1 µL) were spotted onto a 96-well MALDI sample plate and analyzed using a Waters Micromass™ MALDI micro MX™ mass spectrometer and MassLynx™ version 4.1. Data were fitted to the Michaelis-Menten equation using

GraphPad Prism and kinetic parameters were determined from the fit. All assays were performed in triplicate and plotted as mean ± standard deviation.

MS/MS analysis of EF-Tu$_{44-63}$ modified Hyp54

MALDI-TOF mass spectrometry was carried out using a Bruker Ultraflex TOF/TOF mass spectrometer (11). The instrument was calibrated in MS mode directly before data acquisition with Peptide Calibration Standard II (Bruker Daltonics, Coventry, UK) using monoisotopic peptide masses. Peptides were spotted onto a MALDI sample as in PPHD$_{putida}$ kinetic assays. Sample ionization was achieved with a nitrogen laser (337 nm) at 35-45% laser energy and MS/MS spectra were acquired by Laser-induced fragmentation (LIFT)(12).

Amino acid analysis of EF-Tu$_{44-63}$ Hyp54

Amino acid hydrolysates were prepared by exposure of milligram quantities of Hyp54 modified EF-Tu$_{44-63}$ to constant boiling HCl (5.7 M) for 24 h at 110 °C under nitrogen atmosphere and dried by rotary evaporation. Standards were derivatized with 6-aminoquinolyl-*N*-hydroxysuccinimidyl carbamate by mixing amino acid hydrolysate diluted in 0.1 M HCl and derivatizing solution (add 1 mL of 2B AccQTag reagent diluents (acetonitrile) to 2A (AccQTag reagent), vortexed and heated at 55 °C for 10 min. Derivatized amino acids, specifically hydroxyproline, were analyzed against 2 standards (*trans*-3-, *trans*-4-hydroxyproline) on an AccQTag Ultra reversed phase C18 column, 2.1 x 100 mm, particles 1.7 µm (Waters). 1 µL of the sample was injected and separated by linear gradient elution of A [5% (v/v) AccQTag Eluent A)] to B [98.7% acetonitrile, 1.3% (v/v) formic acid], 0-25% over 25 min at a flow rate of 0.7 mL/min at 55 °C. UV detection was performed at a wavelength of 260 nm as described (13). The flow was split at 1:1 ratio before the mass spectrometer. The relative stereochemistry of hydroxyproline was determined by comparison of elution times with the 2 hydroxyproline standards.

MSMS analysis of Pro54/Hyp54 in cells

P. aeruginosa PAO1 wildtype and *P. aeruginosa PA0310* (*PPHD*) deletion strains were grown to stationary phase overnight in LB medium in aerobic (21% O_2) and anaerobic (<0.01% O_2) conditions (for anaerobic growth LB medium was supplemented with KNO_3). Cells were harvested by centrifugation (10,000x*g*; 7 min), resuspended in 1 mL 50 mM HEPES pH 7.5, 200 mM NaCl, lysed by homogenization and the lysate was cleared by centrifugation (18,000x*g*; 10 min). The supernatants were analyzed by SDS-PAGE and the gel band containing EF-Tu was excised and washed twice for 2 hours in 200 µL 50% (v/v) MeOH, 5% (v/v) acetic acid in H_2O, then 200 µL of acetonitrile was added and the gel pieces were dehydrated twice for 5 mins at room temperature and dried in a speedvac. 30 µL of 10 mM dithiothreitol (DTT) in 100 mM NH_4HCO_3 was added and the mixture was incubated for 10 min at room temperature, after which the supernatant was removed. 30 µL of 50 mM iodoacetamide in H_2O was added and the mixture was incubated for 10 min at room temperature, after which the supernatant was removed. 200 µL acetonitrile was added and the gel pieces were dehydrated for 5 mins, after which the supernatant was removed and dried using a Speedvac (Eppendorf). The gel pieces were rehydrated in 100 mM NH_4HCO_3 for 10 min, after which the solution was removed and 200 µL acetonitrile was added and the gel pieces were dried as before. 30 µL of ArgC (2 ng/µL) in 50 mM NH_4HCO_3 was added and the solution was incubated at 37 °C overnight. The peptides were then dried in a speedvac.

Liquid chromatography-tandem mass spectrometry was performed using an Ultimate 3000 nano-HPLC system (Dionex, Sunnyvale, CA, USA) comprising a WPS-3000 micro auto sampler, a FLM-3000 flow manager and column compartment, an LPG-3600 dual-gradient micro-pump, and an SRD-3600 solvent rack controlled by Hystar (Bruker Daltonics, Billerica, MA, USA) and DCMS link 2.0 software. Samples were concentrated on a trapping column Dionex (Sunnyvale, CA, USA), 300 µm i.d., 0.1 cm) at a flow rate of 20 µL/min. For the separation with a C18 Pepmap column (75 µm i.d., 15 cm, Dionex), a flow rate of 250 nL/min was used as generated by a cap-flow splitter cartridge (1/1000). Peptides were eluted by the application of a 30 min multi-step gradient using solvents A (98% H2O, 2% acetonitrile, 0.1% formic acid)

and B (80% acetonitrile, 20% water, 0.1% formic acid): 2-10% B, 0-3 min; 10-25% B, 3-18 min; 25-50% B, 18-30 min, 50-90% B, 30-30.2 min. The liquid chromatography was interfaced directly with a 3D high capacity ion trap mass spectrometer (amaZon; Bruker Daltonics) utilizing 10 µm i.d. distal coated SilicaTips (New Objective, Woburn, MA, USA) and nano-ESI mode. Smart parameter settings (SPS) on the ion trap were tuned for a target mass of 850 *m/z*, compound stability 100% and an ion charge control (ICC) target of 250,000. MS/MS analysis was initiated on a contact closure signal triggered by HyStar software (version 3.2). Up to five precursor ions were selected per cycle with active exclusion (0.5 min) in collision-induced dissociation (CID) mode. CID fragmentation was achieved using helium gas and a 30%–200% collision energy sweep with amplitude 1.0 (ions are ejected from the trap as soon as they fragment).

Raw LC-MS/MS data were processed and Mascot compatible files were created using DataAnalysis 4.0 software (Bruker Daltonics). Database searches were performed using the Mascot algorithm (version 2.4.1) and the UniProt_SwissProt database with bacterial taxonomy restriction (v2013.12.08, number of entries 541,762, after taxonomy filter: 328,677). The following parameters were applied: 2+, 3+ and 4+ ions, peptide mass tolerance 0.3 Da, 13C = 2, fragment mass tolerance 0.6 Da, number of missed cleavages: two, instrument type: ESI-TRAP, fixed modifications: Carbamidomethylation (Cys), variable modifications: Oxidation (Met), Oxidation (Pro).

Production and purification of Hyp54 modified EF-Tu

An *E. coli* BL21(DE3) cell pellet transformed with the pET28a_EF-Tu plasmid (with an *N*-terminal hexahistidine tag) was prepared as described (see protein purification). 10 mg of purified, untagged $PPHD_{putida}$, Fe(II), 2OG, and sodium L-ascorbic acid were added to the cell lysate at a final concentration of 50 µM, 2 mM, and 4 mM, respectively. The cell lysate was allowed to incubate for 1 hour at room temperature and then purification of EF-Tu proceeded as described.

The hydroxylation status of Pro54 was then analyzed by trypsinolysis and MSMS analysis. 1 mg of purified EF-Tu modified Hyp54 was precipitated in $MeOH/CHCl_3$ and dissolved in 100 µL 6 M urea in 100 mM Tris-HCl buffer, pH 7.8 and further diluted in 30 µL of the same buffer. 5 µL 200 mM dithiothreitol (DTT) in 100 mM Tris-HCl buffer, pH 7.8 was added and the mixture was vortexed and incubated for 10 min at room temperature. 30 µL 200 mM iodoacetamide in 100 mM Tris-HCl, pH 7.8 was added and the mixture was vortexed and incubated for 10 min at room temperature. 30 µL 200 mM dithiothreitol (DTT) in 100 mM Tris buffer, pH 7.8 was added and the mixture was vortexed and incubated for an additional 10 min at room temperature. The mixture was diluted with 775 µL MilliQ-H_2O and vortexed. 20 µL trypsin (2 µg/µL in 25 mM Tris-HCl buffer, pH 7.8; Promega, S. aureus V8, MS grade) was added and incubated at 37 °C overnight. The digested peptides were purified and analyzed as described (10).

Binding studies

EF-Tu GTP-GDP turnover experiments were recorded using a Bruker AVIII 700 instrument equipped with a 5 mm inverse cryoprobe and 3 mm MATCH tubes were used throughout (total sample volume 160 µL). Unless otherwise stated, solutions contained 10 µM unmodified or hydroxylated EF-Tu, 50 µM kirromycin, 100 µM GTP, 50 µM *apo*-$PPHD_{putida}$ (where applicable), 100 µM $ZnCl_2$ (where applicable), 100 µM 2OG (where applicable), 10 mM $MgCl_2$ and 200 mM NaCl. Solutions were buffered in 50 mM HEPES pH 7.5 dissolved in 90% H_2O and 10% D_2O. Standard ^1H experiments (16 transients) were used, and water suppression was achieved using the excitation sculpting method (2 ms Sinc1.1000 pulse).

$PPHD_{putida}$ binding constants for 2OG and Mn(II) were determined using a paramagnetic relaxation based NMR technique (14). Mixtures for 2OG binding studies contained 50 µM *apo* (no metal bound) $PPHD_{putida}$, 50 µM $MnCl_2$, 50 µM EF-Tu (full length or $EF\text{-}Tu_{44\text{-}63}$ oligopeptide where applicable), 10 mM $MgCl_2$ and 200 mM NaCl. Solutions were buffered using ~30 mM Tris-d11 and ~20 mM HEPES pH 7.5 dissolved in 36.25% H_2O and 63.75% D_2O. Experiments were recorded using a Bruker AVII 500 instrument equipped with a 5 mm inverse TXI probe and 3 mm MATCH tubes were used throughout (total sample volume 160 µL). Saturation recovery ($90^\circ_x–G_1–90^\circ_y–G_2–90^\circ_x–G_3–\tau–acq$) experiments were performed with 1 scan with a relaxation delay of at least 5 times T_1 between transients. The gradient pulses were achieved

using a 1 ms Sinebell gradient pulse (G_1 = 40%; G_2 = 27.1%; G_3 = 15%). The receiver gain was set to minimum value (rg = 1) to prevent receiver overload. Typically, 10 delay points varied between 100 ms and 60 s were used. T_1 values were obtained using the *Bruker T1/T2 Relaxation* option and peak area was used for curve fitting. The titrant (typically ~0.2 µL) was added using a 1 µL plunger-in-needle syringe (SGE) and sample mixing was conducted using a 250 µL gas tight syringe (SGE). Binding constants were obtained by non-linear curve fitting using OriginPro 8.0 (OriginLab) with the equation as described (15).

PPHD-Mn(II) binding experiments were performed in the same manner as 2OG-binding experiments, except that the mixture contained 25 µM $MnCl_2$, 62.5 µM EF-Tu (unhydroxylated or modified Hyp54 where applicable), 10 mM $MgCl_2$, and 200 mM NaCl. The titrant was *apo* $PPHD_{putida}$. Solutions were buffered using ~40 mM Tris-d11 and ~10 mM HEPES pH 7.5 dissolved in 18.75% H_2O and 81.25% D_2O.

$ZnCl_2$ inhibition experiments were performed similar to EF-Tu GTP-GDP turnover experiments: Mixture contained 10 µM *apo* $PPHD_{putida}$, 50 µM $FeCl_2$, 500 µM 2OG, 600 µM EF-Tu_{44-63} (H_2N-IVEFDKIDSAPEEKARGITI-$CONH_2$), 400 µM ZnCl2 (where applicable), 1.25 mM ascorbate and 100 mM NaCl. Solutions were buffered using 50 mM Tris-D11 (pH 7.5) dissolved in 90% H_2O and 10% D_2O. Standard ^1H experiments (16 transients) were used, and water suppression was achieved using the excitation sculpting method (2 ms Sinc1.1000 pulse).

Calculation of ΔG_{bind} for PPHD:EF-Tu complex

For the calculations on the $PPHD_{putida}$:EF-Tu protein-protein binding free energy, ΔG_{bind} was decomposed into protein-protein binding energy in vacuum (ΔG_{int}) and solvation energy (ΔG_{solv}) during complexation. $\Delta G_{bind} = \Delta G_{\text{int}} + \Delta G_{solv}$ where: $\Delta G_{\text{int}} = \Delta E_{\text{int}\,ra} + \Delta E_{elec} + \Delta E_{vdw} - T\Delta S_{trans} - T\Delta S_{rot} - T\Delta S_{vib}$ and

$$\Delta G_{solv} = \Delta G_s((P_{pphd} \cdot P_{ef-tu})_{complex}) - \Delta G_s(P_{pphd}) - \Delta G_s(P_{ef-tu}) \quad .$$

$\Delta E_{\text{int}\,ra}$ represents the change of energy associated with bond stretching, angle and proper, improper torsions. ΔE_{elec} and ΔE_{vdw} represent electrostatic potential and van der waals potential respectively. Entropic contributions can be described with translational, rotational and vibrational entropies at 300K, respectively. To find energy minimization minima, each protein and protein complex were relaxed through 3000 steps of energy minimization using the basis Newton-Raphson (ABNR) algorithm.

$$S_{trans} = \frac{k_B}{2}[5 + 3\ln(\frac{2\pi m}{\beta h^2}) - 2\ln\rho]$$

$$S_{rotation} = \frac{k_B}{2}[3 + \ln(\pi I_A I_B I_C) + 3\ln(\frac{8\pi^2}{\beta h^2}) - 2\ln\sigma]$$

$$S_{vib} = \sum_i k_B[\frac{\beta h\nu_i}{e^{\beta h\nu_i} - 1} - \ln(1 - e^{-\beta h\nu_i})] \ .$$

Where m is mass of a protein, $\beta = 1/k_B T$, h is Planck constant, ρ is number of density (in unit of M), σ is symmetry factor of the molecule, $I_A I_B I_C$ is three rotational moment of inertia and ν_i is normal mode frequency (16). Solvation free energies (ΔG_{solv}) were calculated with Generalized Born method (GBSA/IM) implemented in CHARMM based on Solvent Accessible Surface Area (SASA) of each atom, using atomic solvation parameters (17). ΔS_{trans} and ΔS_{rot} can be calculated from mass and moment of inertia. ΔS_{vib}

were calculated from the full sets of internal normal mode frequencies using the distance dependent dielectric constant. Overall, binding free energy of protein complex shows $\Delta G_{bind} = -9.7 kcal/mol$ comprising -22.7 kcal/mol for ΔG_{int} and 13.0 kcal/mol for ΔG_{solv}.

Identification of putative proly-hydroxylase orthologs, multiple-sequence alignment and phylogenetic tree construction

Using human prolyl-hydroxylase genes *EGLN1* (UniProt accession number Q9GZT9), *LEPRE1* (Q32P28), *OGFOD1* (Q8N543), and *P4HA1* (P13674) and the human lysyl-hydroxylase gene *PLOD1* (Q02809) as query sequences, Uniprot (http://www.uniprot.org/) and Genbank (https://www.ncbi.nlm.nih.gov/genbank/) were searched for putative prolyl-hydroxylase orthologs in the major taxonomic groups from the tree of life. Two conserved Pfam (18) domains, 2OG-FeII_Oxy (PF03171) and 2OG-FeII_Oxy_3 (PF13640), were identified among the queried sequences and the protein set containing these domains was downloaded from one representative species for each major taxonomic group across the Tree of Life using the Uniprot Batch tool. These results were validated by searching Genbank using Delta BLAST (default parameters) with the same query sequences (19). In general, there was agreement between Uniprot-identified and Genbank-identified sequences for most groups, but four additional phyla containing putative orthologous sequences were identified using Delta BLAST: Cryptophyta, Haptophyceae, Rhizaria and Rhodophyta. To isolate putative orthologous sequences from these groups, the proteomes from whole-genome sequenced organisms corresponding to each group were obtained: *Guillardia theta* (Genbank accession number PRJNA223305), *Emilianaia huxleyi* (PRJNA222302), *Reticulomyxa filosa* (PRJNA29155) and *Galdieria sulphuraria* (PRJNA221242). The Pfam Batch search tool, using the default Gathering Threshold, was used to identify and download sequences containing the aforementioned domains.

The hidden-markov model (HMM) profiles were obtained for both domains, 2OG-FeII_Oxy (PF03171) and 2OG-FeII_Oxy_3 (PF13640), and HMMER3 hmmalign (http://hmmer.janelia.org/) was used to perform a domain alignment on the corresponding proteins sets. The domain-alignments were trimmed to include all domain-aligned amino acid residues in addition to 20aa up- and down-stream residues. To minimize homology missalignments, sequences not containing the two conserved histidine residues characteristic of the 2OG-Fe(II) oxygenase family members metal-binding HXD…H motif were removed (thus, we may have excluded 2OG oxygenases not containing these motifs). Both domain-alignments were then combined in a single FASTA file and all sequences were realigned using MAFFT (Parameters: L-INS-i, BLOSUM45, Gap opening penalty 2, Offset value 0.5, Unalign level 0.2)(20). To remove regions of ambiguous alignment, Trimal (21) was used to retain only those sites in which greater than or equal to 90% of the sequences contained an amino acid. Non-unique sequences were removed using ElimDupes (http://hcv.lanl.gov/content/sequence/ELIMDUPES/elimdupes.html). The resulting alignment contained 89 sites across 278 sequences.

The alignment was used to infer a gene tree using the program FastTree (22), under the WAG model of amino acid evolution. Branch support values were obtained with the Shimodaira-Hasegawa test (23). The tree was edited with iTOL (24) and arbitrarily rooted in the Alpha-ketoglutarate-dependent dioxygenase (AlkB) group to ease reading of the tree.

SI References

1. Winn MD, et al. (2011) Overview of the CCP4 suite and current developments. *Acta Crystallogr D Biol Crystallogr* 67(Pt 4):235-242.
2. Minor W, Cymborowski M, Otwinowski Z, & Chruszcz M (2006) HKL-3000: the integration of data reduction and structure solution - from diffraction images to an initial model in minutes. *Acta Crystallogr D Biol Crystallogr* 62:859-866.
3. Kabsch W (2010) Xds. *Acta Crystallogr D Biol Crystallogr* 66(Pt 2):125-132.
4. Kabsch W (2010) Integration, scaling, space-group assignment and post-refinement. *Acta Crystallogr D Biol Crystallogr* 66(Pt 2):133-144.
5. McCoy AJ, et al. (2007) Phaser crystallographic software. *J Appl Crystallogr* 40(Pt 4):658-674.
6. Adams PD, et al. (2010) PHENIX: a comprehensive Python-based system for macromolecular structure solution. *Acta Crystallogr D Biol Crystallogr* 66(Pt 2):213-221.
7. Emsley P & Cowtan K (2004) Coot: model-building tools for molecular graphics. *Acta Crystallogr D Biol Crystallogr* 60(Pt 12 Pt 1):2126-2132.
8. Jacobs MA, et al. (2003) Comprehensive transposon mutant library of Pseudomonas aeruginosa. *Proc Natl Acad Sci USA* 100(24):14339-14344.
9. Essar DW, Eberly L, Hadero A, & Crawford IP (1990) Identification and characterization of genes for a second anthranilate synthase in Pseudomonas aeruginosa: interchangeability of the two anthranilate synthases and evolutionary implications. *J Bacteriol* 172(2):884-900.
10. Aik W, et al. (2014) Structure of human RNA N6-methyladenine demethylase ALKBH5 provides insights into its mechanisms of nucleic acid recognition and demethylation. *Nucleic Acids Res* 42(7):4741-4754.
11. Suckau D, et al. (2003) A novel MALDI LIFT-TOF/TOF mass spectrometer for proteomics. *Anal Bioanal Chem* 376(7):952-965.
12. Macht M, Asperger A, & Deininger SO (2004) Comparison of laser-induced dissociation and high-energy collision-induced dissociation using matrix-assisted laser desorption/ionization tandem time-of-flight (MALDI-TOF/TOF) for peptide and protein identification. *Rapid Commun Mass Spectrom* 18(18):2093-2105.
13. Ge W, et al. (2012) Oxygenase-catalyzed ribosome hydroxylation occurs in prokaryotes and humans. *Nat Chem Biol* 8(12):960-962.
14. Leung IKH, Flashman E, Yeoh KK, Schofield CJ, & Claridge TDW (2010) Using NMR Solvent Water Relaxation to Investigate Metalloenzyme-Ligand Binding Interactions. *J Med Chem* 53(2):867-875.
15. Morton CJ, et al. (1996) Solution structure and peptide binding of the SH3 domain from human Fyn. *Structure* 4(6):705-714.
16. Tidor B & Karplus M (1994) The contribution of vibrational entropy to molecular association. The dimerization of insulin. *J Mol Biol* 238(3):405-414.
17. Spassov VZ, Yan L, & Szalma S (2002) Introducing an implicit membrane in generalized Born/solvent accessibility continuum solvent models. *J Phys Chem B* 106(34):8726-8738.
18. Punta M, et al. (2012) The Pfam protein families database. *Nucleic Acids Res* 40(Database issue):D290-301.
19. Boratyn GM, et al. (2012) Domain enhanced lookup time accelerated BLAST. *Biol Direct* 7:12.
20. Katoh K & Standley DM (2013) MAFFT multiple sequence alignment software version 7: improvements in performance and usability. *Mol Biol Evol* 30(4):772-780.
21. Capella-Gutierrez S, Silla-Martinez JM, & Gabaldon T (2009) trimAl: a tool for automated alignment trimming in large-scale phylogenetic analyses. *Bioinformatics* 25(15):1972-1973.
22. Price MN, Dehal PS, & Arkin AP (2010) FastTree 2--approximately maximum-likelihood trees for large alignments. *PLoS One* 5(3):e9490.
23. Shimodaira H & Hasegawa M (1999) Multiple comparisons of log-likelihoods with applications to phylogenetic inference. *Mol Biol Evol* 16(8):1114-1116.

24. Letunic I & Bork P (2011) Interactive Tree Of Life v2: online annotation and display of phylogenetic trees made easy. *Nucleic Acids Res* 39:W475-W478.
25. Das T & Manefield M (2012) Pyocyanin promotes extracellular DNA release in Pseudomonas aeruginosa. *PLoS One* 7(10):e46718.
26. Yang L, et al. (2007) Effects of iron on DNA release and biofilm development by Pseudomonas aeruginosa. *Microbiology* 153(Pt 5):1318-1328.
27. Petrova OE, Schurr JR, Schurr MJ, & Sauer K (2011) The novel Pseudomonas aeruginosa two-component regulator BfmR controls bacteriophage-mediated lysis and DNA release during biofilm development through PhdA. *Mol Microbiol* 81(3):767-783.
28. Chowdhury R, et al. (2009) Structural basis for binding of hypoxia-inducible factor to the oxygen-sensing prolyl hydroxylases. *Structure* 17(7):981-989.
29. Koski MK, et al. (2009) The Crystal Structure of an Algal Prolyl 4-Hydroxylase Complexed with a Proline-rich Peptide Reveals a Novel Buried Tripeptide Binding Motif. *J Biol Chem* 284(37):25290-25301.
30. Kim HS, et al. (2010) Crystal structure of Tpa1 from Saccharomyces cerevisiae, a component of the messenger ribonucleoprotein complex. *Nucleic Acids Res* 38(6):2099-2110.
31. Trewick SC, Henshaw TF, Hausinger RP, Lindahl T, & Sedgwick B (2002) Oxidative demethylation by Escherichia coli AlkB directly reverts DNA base damage. *Nature* 419(6903):174-178.
32. Falnes PO, Johansen RF, & Seeberg E (2002) AlkB-mediated oxidative demethylation reverses DNA damage in Escherichia coli. *Nature* 419(6903):178-182.

Table S1. Crystallization conditions.

	PPHD:NOG	EF-Tu:GDP	PPHD:EF-Tu complex
Protein solution	~10 mg/mL PPHD, 2 mM $MnCl_2$, 5 mM NOG, 5 mM $EF\text{-}Tu_{44\text{-}63}$	~18 mg/mL EF-Tu, 0.05 M HEPES pH 7.5, 10 m	~15 mg/mL PPHD:EF-Tu, 0.8 mM $MnCl_2$, 0.9 mM NOG
Reservoir solution	0.1 M MIB buffer pH 5.0, 25% (w/v) PEG 1500	0.05 M MES pH 5.6, 0.1 M MgOAc, 20% (v/v) MPD, 10 mM $SrCl_2$	0.1 M HEPES pH 7.5, 0.1 M $MgCl_2$, 22% (w/v) polyacrylate 5100, 1 mM GDP

Table S2. Crystallographic data and refinement statistics.

	PPHD:NOG	EF-Tu:GDP	PPHD:EF-Tu complex
X-ray source	Diamond Light Source beamline I04	Diamond Light Source beamline I03	Diamond Light Source beamline I04
Wavelength (Å)	0.97950	0.97630	0.97950
PDB Acquisition Code	4J25	4J0Q	4IW3
Resolution (Å)	1.97 (2.02–1.97)§	2.29 (2.38–2.29)§	2.70 (2.84-2.70)§
Space group	*P* 1	*C* 1 2 1	*P* 3_1 2 1
Unit Cell Dimensions (*a* Å, *b* Å, *c* Å)	45.33 62.16 132.83	212.51 155.62 99.3	200.70 200.70 74.83
Molecules per a.u.	8	5	4 (2 PPHD; 2 EF-Tu)
Total Number of Reflections Observed	383204	856176	438242
Number of Unique Reflections	99718 (7268)§	129510 (12208)§	47866 (6913)§
Redundancy	3.8 (3.9)§	6.6 (5.6)§	9.1 (8.2)§
Completeness (%)	97.7 (96.7)§	99.3 (93.9)§	99.9 (99.2)§
Wilson B	27.8	64.1	74.7
$I/\sigma(I)$	10.6 (2.3)§	30.2 (1.7)§	13.4 (1.7)§
§§R_{merge}	0.069	0.056	0.086
*R_{cryst}	0.219	0.174	0.168
†R_{free}	0.257	0.213	0.218
¶RMS deviation	0.009 (1.0°)	0.01 (1.3°)	0.01 (1.2°)
Average *B* factors (Å^2)	34.1	67.1	60.2
Number of Water Molecules	563	316	166

§ Parentheses indicate high resolution shell

§§ $R_{merge} = \sum_j \sum_h | I_{hj} - \langle I_h \rangle | / \sum_j \sum_h \langle I_h \rangle \times 100$

***** $R_{cryst} = \sum ||Fobs| - |Fcalc|| / |Fobs| \times 100$

† R_{free}, based on 2-5% of the total reflections

¶ RMS deviation from ideality for bonds (followed by the value for angles).

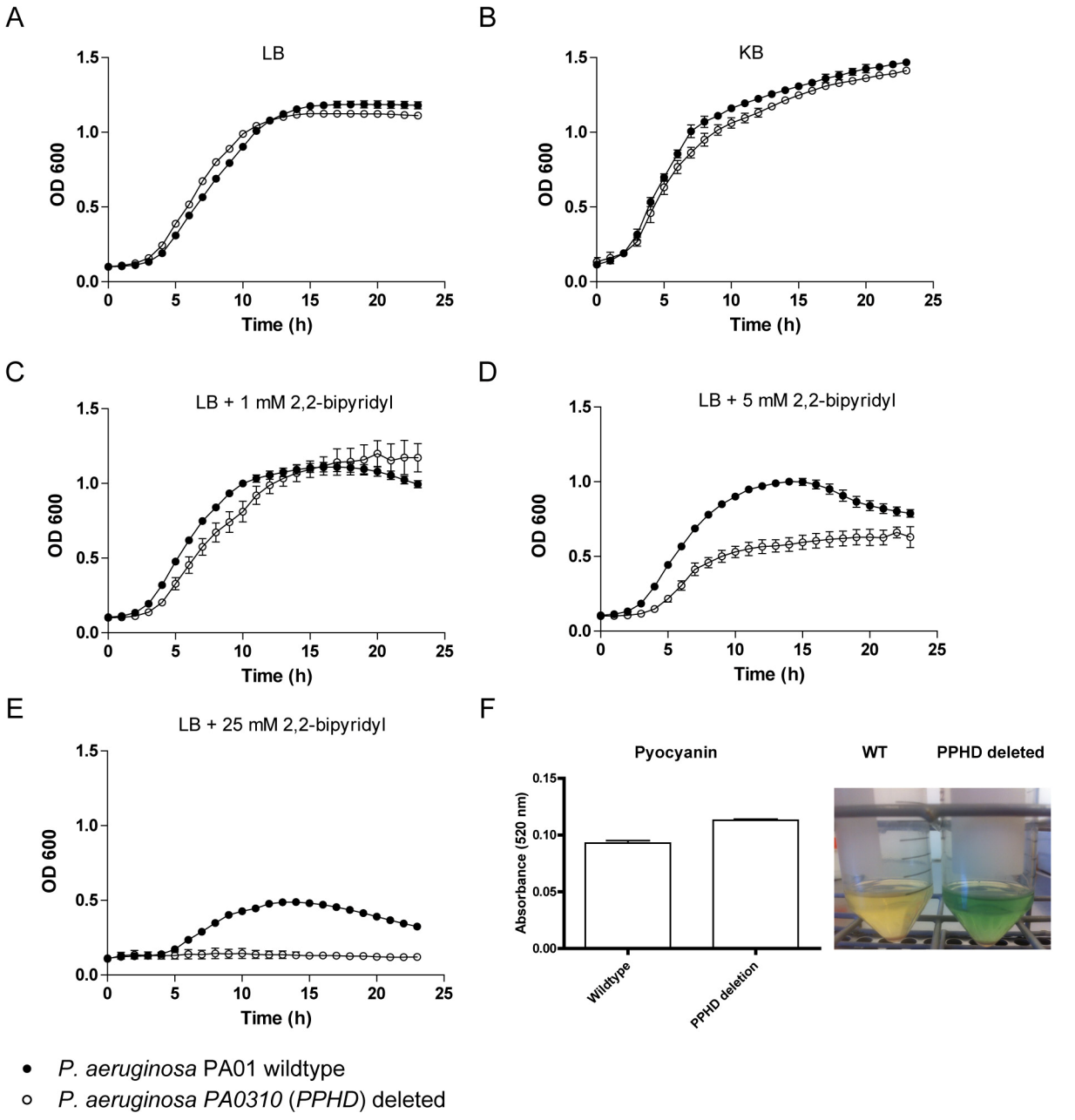

Fig. S1. A *P. aeruginosa* PPHD deleted strain displays limited growth in the presence of iron-chelators and increased production of pyocyanin. Growth curves of *P. aeruginosa* wildtype and *PA0310* (*PPHD*) knockout in (*A*) LB (Luria Broth) and (*B*) King's Broth (KB) and (*C, D, E*) in LB and the presence of 2,2-bipyridine revealing inhibited growth in the PPHD deleted strain. (*F*) *P. aeruginosa* PPHD deleted strain produces more pyocyanin, as shown by the appearance of a green color (9). The observed decrease in OD_{600} over time in *P. aeruginosa* is interesting because autolysis and extracellular DNA (eDNA) release has been shown to be affected by pyocyanin and iron availability (25-27). All data are shown as the mean (n=3) ± standard deviation (SD).

Table S3. Interaction studies of hexahistidine-tagged $PPHD_{putida}$ in *P. putida* reveals possible association between $PPHD_{putida}$ and EF-Tu. The higher protein score suggests increased abundance and confidence. Peptide number, peptide score and sequence refer to number of peptides identified per protein and relative number of *b*/*y* ions matched per representative peptide. Q88CM1 refers to $PPHD_{putida}$. See Materials and Methods for details.

Uniprot Accession	Protein name	Gene Name	Protein Score	Peptide Number	Peptide Score	Peptide Sequence
Q88QN7	Elongation factor Tu-B	*tufB*	854	104	36.09	LLDEGR
Q88QP8	Elongation factor Tu-A	*tufA*	685	104	36.09	LLDEGR
Q88CM1	Putative uncharacterized protein	*PP_5159*	836	135	28.45	ALAAECR
Q88BZ2	Putative uncharacterized protein	*PP_5391*	340	2088	1.91	MAAAKTPEAR
Q88JK1	Universal stress protein family	*PP_2648*	176	89	0.73	TIELAK
Q88QN6	30S ribosomal protein S10	*rpsJ*	146	7212	79.74	LIDQSTQEIVETAKR
Q88PS2	Peptidyl-prolyl cis-trans isomerase	*slyD*	117	166	8.38	MLIAANK
Q88DZ0	Ketol-acid reductoisomerase	*ilvC*	78	2486	0.68	NEIEPNIKK
Q88QM9	30S ribosomal protein S3	*rpsC*	78	225	8.29	AVQNAMR
Q88EH2	Pterin-4-alpha-carbinolamine dehydratase	*phhB*	73	1235	2.72	VAETAEGRK
Q88MI0	30S ribosomal protein S2	*rpsB*	54	1290	9.32	IHIVNLEK
Q88QM2	30S ribosomal protein S14	*rpsN*	38	4485	16.48	LTGRPHGVYRK
Q88KB0	Putative uncharacterized protein	*PP_2380*	37	3208	1.57	EVKAIELPAGK
Q88MP1	2,3,4,5-tetrahydropyridine-2,6-dicarboxylate N-succinyltransferase	*dapD*	36	1981	2.05	NSLNGAVECK
Q88BZ1	Putative uncharacterized protein	*PP_5392*	35	882	15.77	IFDLEQR

Table S4. Table of peptides based on *P. putida* EF-Tu (Uniprot: Q88QP8) that were screened for $PPHD_{putida}$ dependent hydroxylation. The 14 distinct peptides encompass all 19 prolines in the EF-Tu sequence. Methionines were mutated to other amino acid residues in order to avoid potential false positives due to methionine oxidation in the mass spectrometer. All peptides were synthesized to produce a *C*-terminal amide residue.

Peptide Sequence	Residue Range	Mutations from native EF-Tu	Hydroxylation Observed
AKEKFDRSL**P**HVNVGTIGH	2-20	-	NO
IVEFKIDSA**P**EEKARGITI	44-63	-	**YES**
HYAHVDC**P**GHADYVKNLITG	76-95	M92L	NO
ILVCSAADG**P**A**P**QTREHILL	103-122	M113A	NO
LLSRQVGV**P**YIVVFLNKADL	121-140	-	NO
DLLSTYDF**P**GDDT**P**IIIGSA	156-175	-	NO
VETLDAYI**P**E**P**VRAIDQ**P**FL	196-215	S201A	NO
PVRAIDQ**P**FLL**P**IEDVFSIS	206-225	M216L	NO
ERGIVRVQD**P**LEIVGLRDTT	236-255	-	NO
ERGQVLVK**P**GSVK**P**HTKFTA	291-310	-	NO
SKEEGGRHT**P**FFKGYR**P**QFY	316-335	-	NO
GRHT**P**FFKGYR**P**QFYFRTTD	321-340	-	NO
VTGNCEL**P**EGVELVL**P**GDNI	341-360	M353L, M355L	NO
EL**P**EGVEAVA**P**GDNIQLTVT	346-365	M353A, M355A, M362L	NO

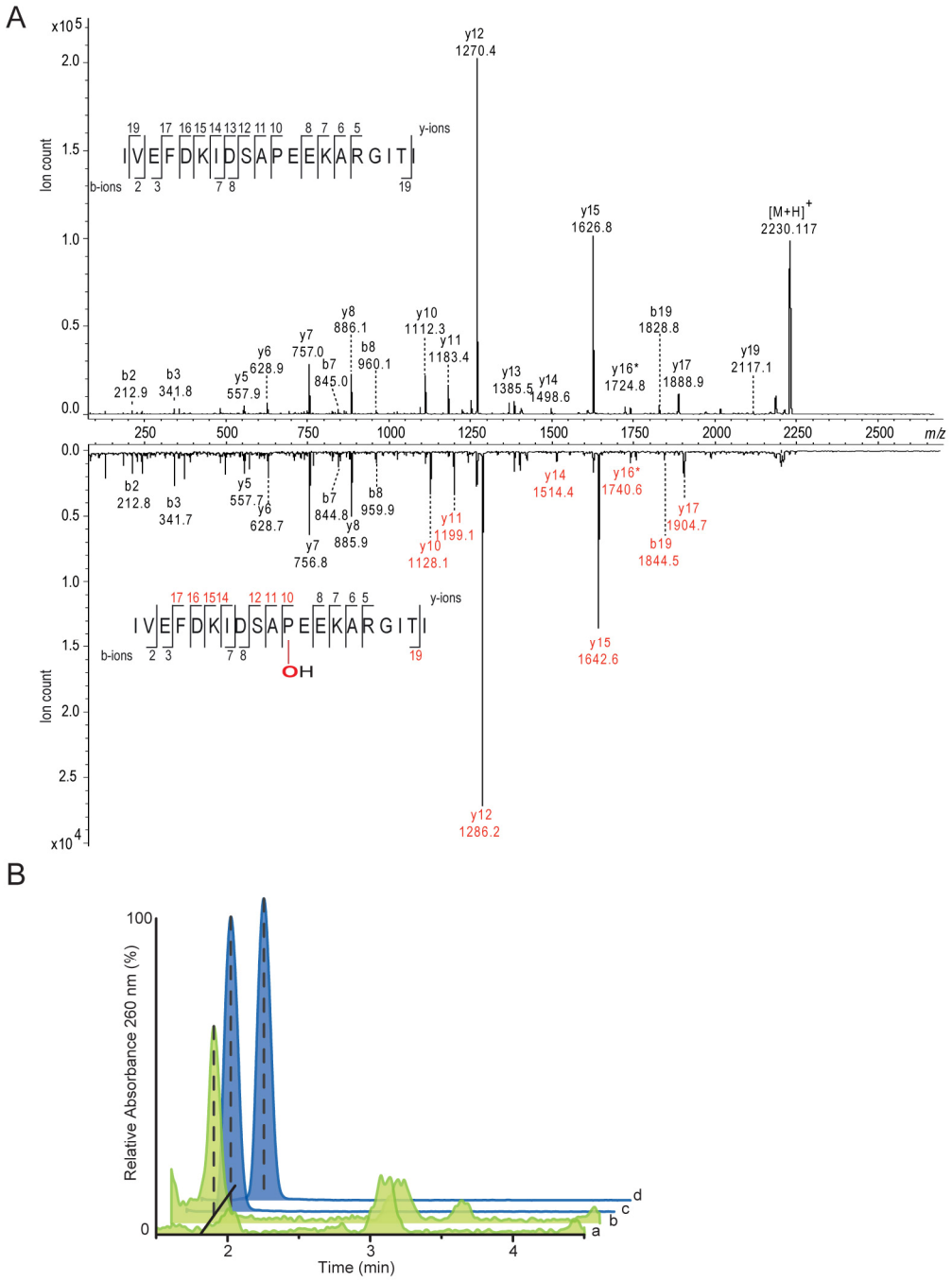

Fig. S2. PPHD*putida* catalyzes *trans*-4 prolyl-hydroxylation of EF-Tu Pro54. (*A*) MS/MS analysis of PPHD*putida* treated and untreated EF-Tu$_{44\text{-}63}$ confirms hydroxylation at Pro54 (Hyp54). (*B*) Amino-acid analyses demonstrates that PPHD*putida* hydroxylates EF-Tu$_{44\text{-}63}$ oligopeptide substrate at Pro54 in 4-*trans* (2*S*,4*R*) stereochemistry. a**:** EF-Tu$_{44\text{-}63}$ control; b: EF-Tu$_{44\text{-}63}$ modified Hyp54; c: *trans*-4-hydroxyproline standard; d: *trans*-3-hydroxyproline standard.

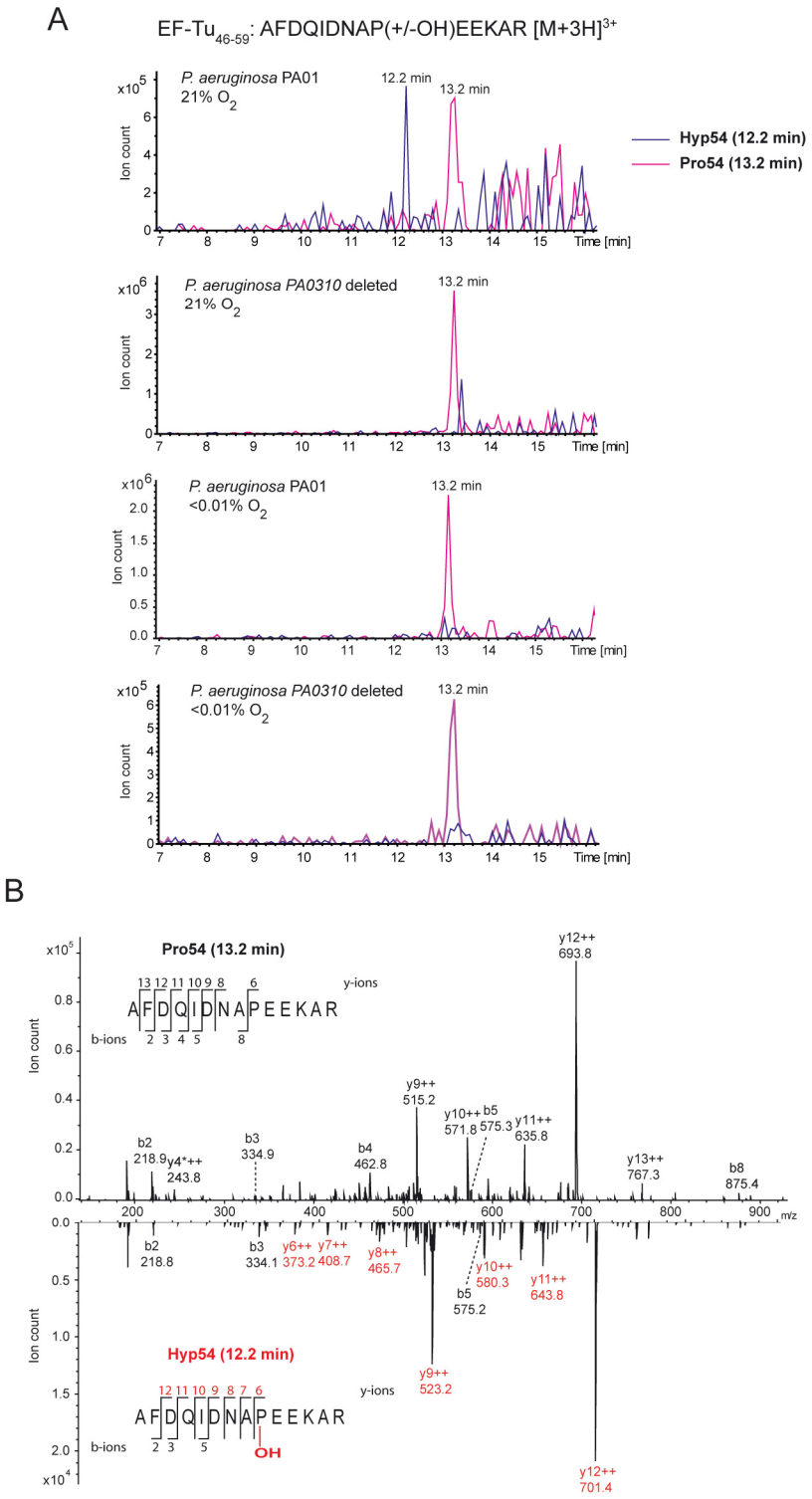

Fig. S3. Hydroxylation of EF-Tu at Pro54 is catalyzed by PPHD in cells. (*A*) Extracted ion chromatograms (EICs) and (*B*) associated MS/MS analyses of *P. aeruginosa* PAO1 wildtype and *PA0310* (PPHD) deleted strains grown in aerobic (21% O_2) and anaerobic (<0.01% O_2) conditions demonstrates EF-Tu Pro54 is hydroxylated in cells in the wildtype but not the deleted strain in an oxygen dependent manner (*m/z* 535.25 and *m/z* 540.59 correspond to Pro54 and Hyp54, respectively).

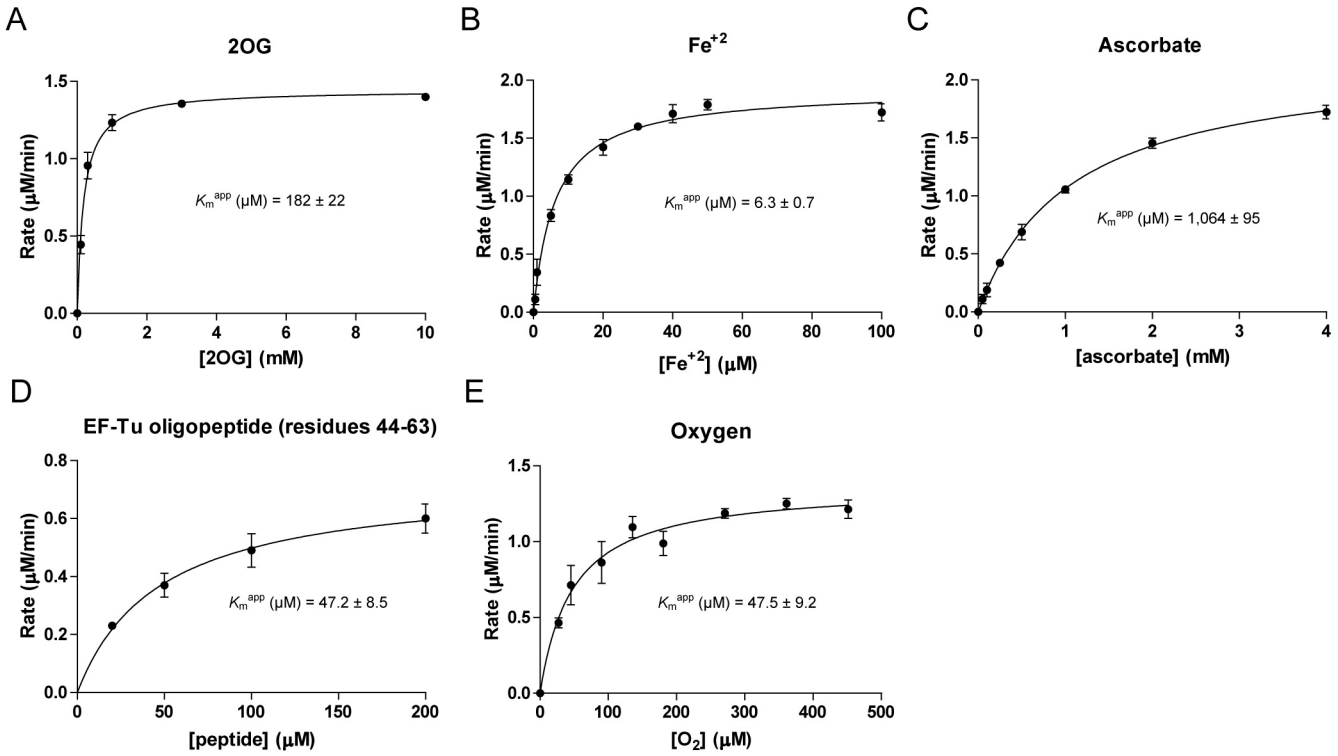

Fig. S4. PPHD$_{putida}$ K_m^{app} determination for (*A*) 2OG (*B*) Fe(II) (*C*) sodium L-ascorbate (*D*) EF-Tu$_{44-63}$ and (*E*) oxygen. All data are shown as the mean (n=3) ± standard deviation (SD).

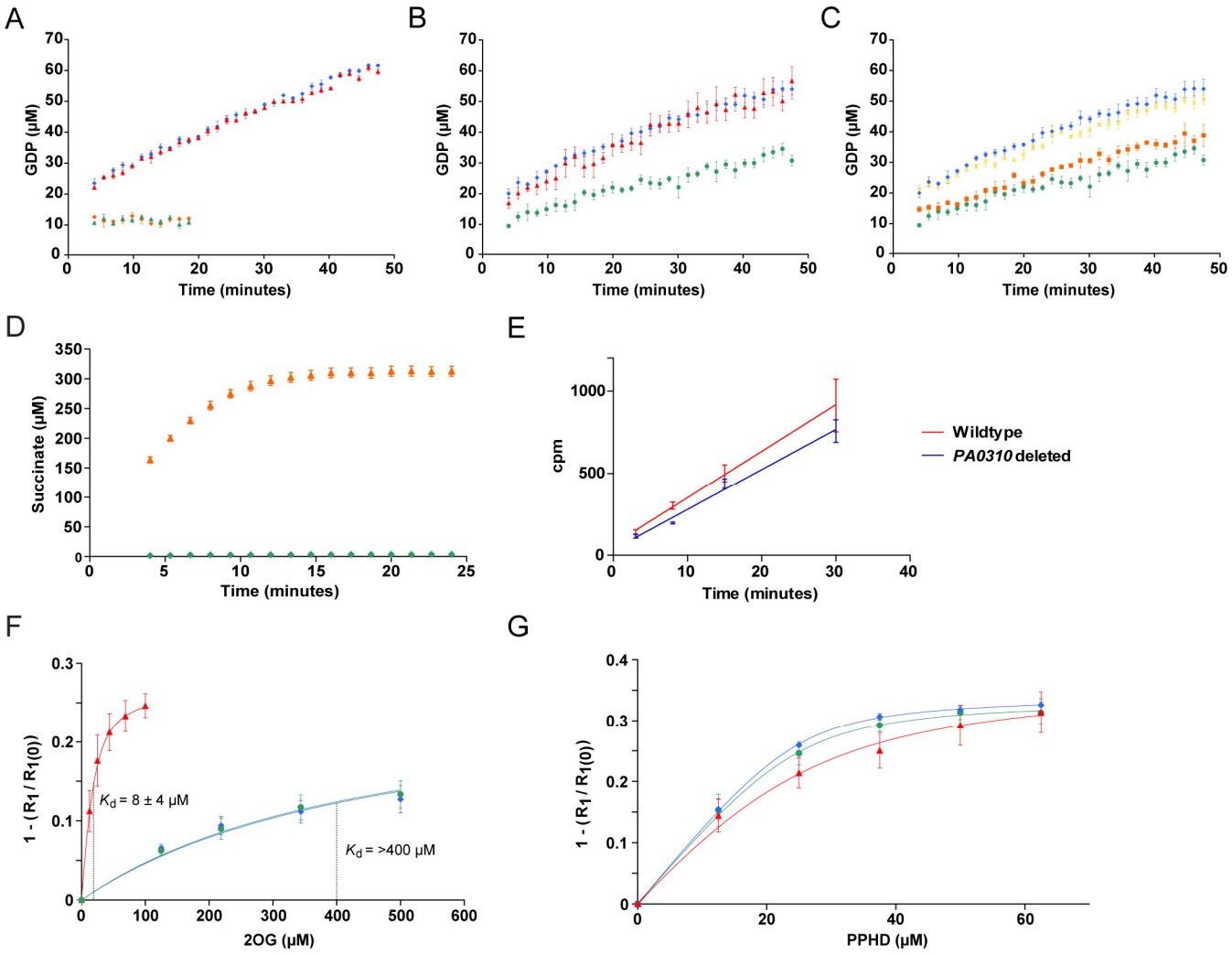

Fig. S5. ^{1}H NMR monitoring of EF-Tu GTP hydrolysis. (*A*) EF-Tu catalyzed GTP to GDP turnover is kirromycin dependent: ◆ EF-Tu with kirromycin; ▲ EF-Tu Hyp54 with kirromycin; ◆ EF-Tu without kirromycin; ▲ EF-Tu Hyp54 without kirromycin. (*B*) EF-Tu catalyzed GTP to GDP turnover as monitored by ^{1}H NMR. The observed rate of EF-Tu mediated GTP hydrolysis is approximately halved in the presence of PPHD-Zn(II)-2OG: ◆ EF-Tu only; ● EF-Tu in the presence of PPHD-Zn(II)-2OG; ▲ EF-Tu Hyp54 in the presence of PPHD-Zn(II)-2OG. (*C*) The rate of GTP hydrolysis is dependent on the presence of Zn(II) and 2OG in the PPHD$_{putida}$ active site: ◆ EF-Tu only; ● EF-Tu in the presence of PPHD-Zn(II)-2OG; ■ EF-Tu in the presence of PPHD-Zn(II); × EF-Tu in the presence of isolated PPHD. (*D*) PPHD$_{putida}$ activity is inhibited by $ZnCl_2$ as monitored by ^{1}H NMR (2OG oxidation into succinate is measured): ▲ no $ZnCl_2$ added; ● 400 μM $ZnCl_2$ added. (*E*) Growth of *P. aeruginosa* PAO1 wildtype and *PA0310* (*PPHD*) deleted strains reveals no apparent effect on relative global translation as measured by ^{35}S-methionine incorporation. (*F*) Measurement of the PPHD$_{putida}$ 2OG K_d by NMR (14) in the presence of EF-Tu protein (8 ± 4 μM)(▲) compared to the absence of any substrate (>400 μM)(◆) and in the presence of EF-Tu$_{44\text{-}63}$ (>400 μM)(●). (*G*) In the absence of 2OG, addition of unhydroxylated EF-Tu$_{protein}$ weakens metal [Mn(II)] binding to PPHD$_{putida}$. K_d of Mn(II) to PPHD in the absence of any substrate (◆)(2 ± 0.5 μM), in the presence of unhydroxylated EF-Tu protein (▲)(8 ± 3 μM), and in the presence of EF-Tu Hyp54 (●)(2 ± 1 μM). All data are shown as the mean (n=3) ± standard deviation (SD).

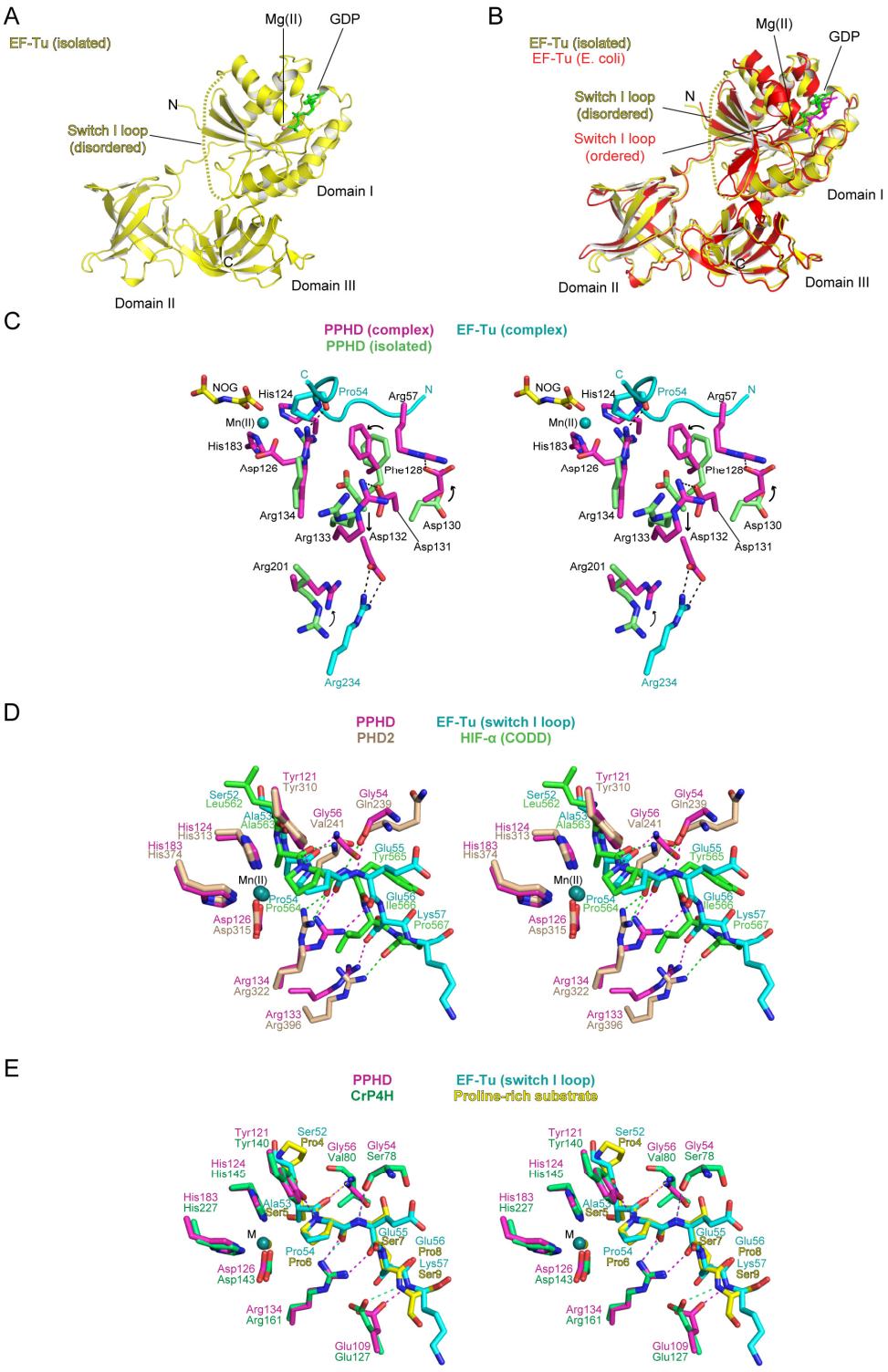

Fig. S6. Views from a crystal structure of isolated *P. putida* EF-Tu and comparison with *E. coli* EF-Tu. (*A*) View from the overall structure of *P. putida* EF-Tu (yellow) in its GDP-bound conformation with the switch I loop disordered (residues 44-59; dotted line). (*B*) Superimposition of *P. putida* EF-Tu (yellow) with *E. coli* EF-Tu (red)(PDB ID: 1DG1)(r.m.s.d. 1.5 Å over 353 Cα atoms). (C) Wall-eyed stereo view of main text Fig. 3*F*. (*D*) Wall-eyed stereo view of main text Fig. 4*A*. (*E*) Wall-eyed stereo view of main text Fig. 4*B*.

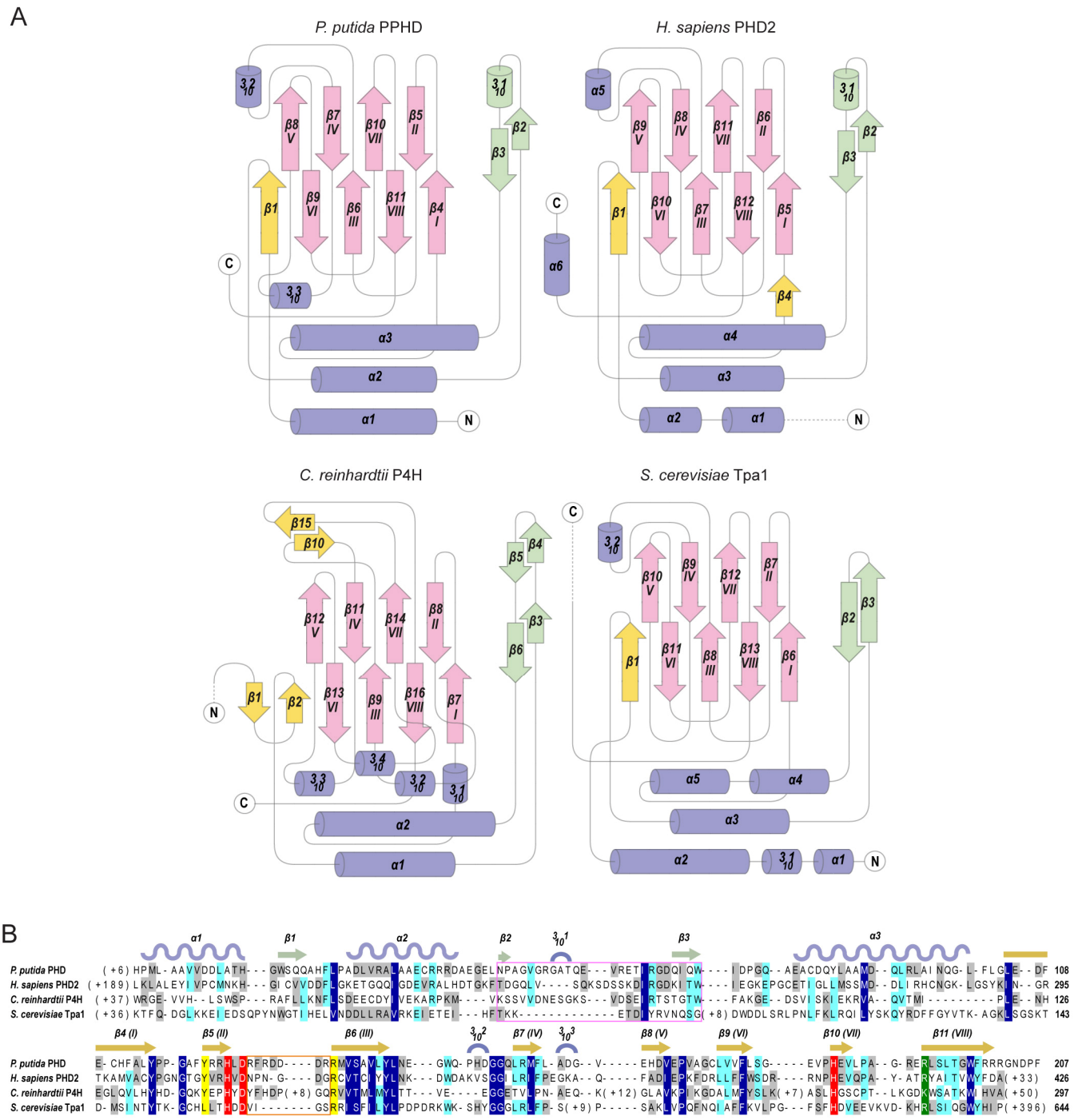

Fig. S7. Structural analyses of prolyl-4- and prolyl-3-hydroxylases. (*A*) Topology diagrams of representative prolyl-hydroxylases from different subfamilies reveal structural similarities between catalytic domains. Colors represent structural homology to PPHD$_{putida}$; α-helix and 3_{10}-helix (blue), DSBH β-strands (pink), β2-β3 finger loop (green), other β-strands (yellow). (*B*) Structure-based sequence alignments of prolyl-hydroxylases for which crystal structures are reported. *Pseudomonas putida* PHD (PDB ID: 4IW3), *Homo sapiens* PHD2 (PDB ID: 3HQR)(28), *Chlamydomonas reinhardtii* P4H (PDB ID: 3GZE)(29), and *Saccharomyces cerevisiae* Tpa1 (PDB ID: 3KT4)(30); secondary structure is derived from *P. putida* PPHD; β2-β3 finger loop (magenta box) and β5(II)-β6(III) thumb loop (orange box); metal-binding residues (red), 2OG-binding residue (green), substrate-binding residues (yellow).

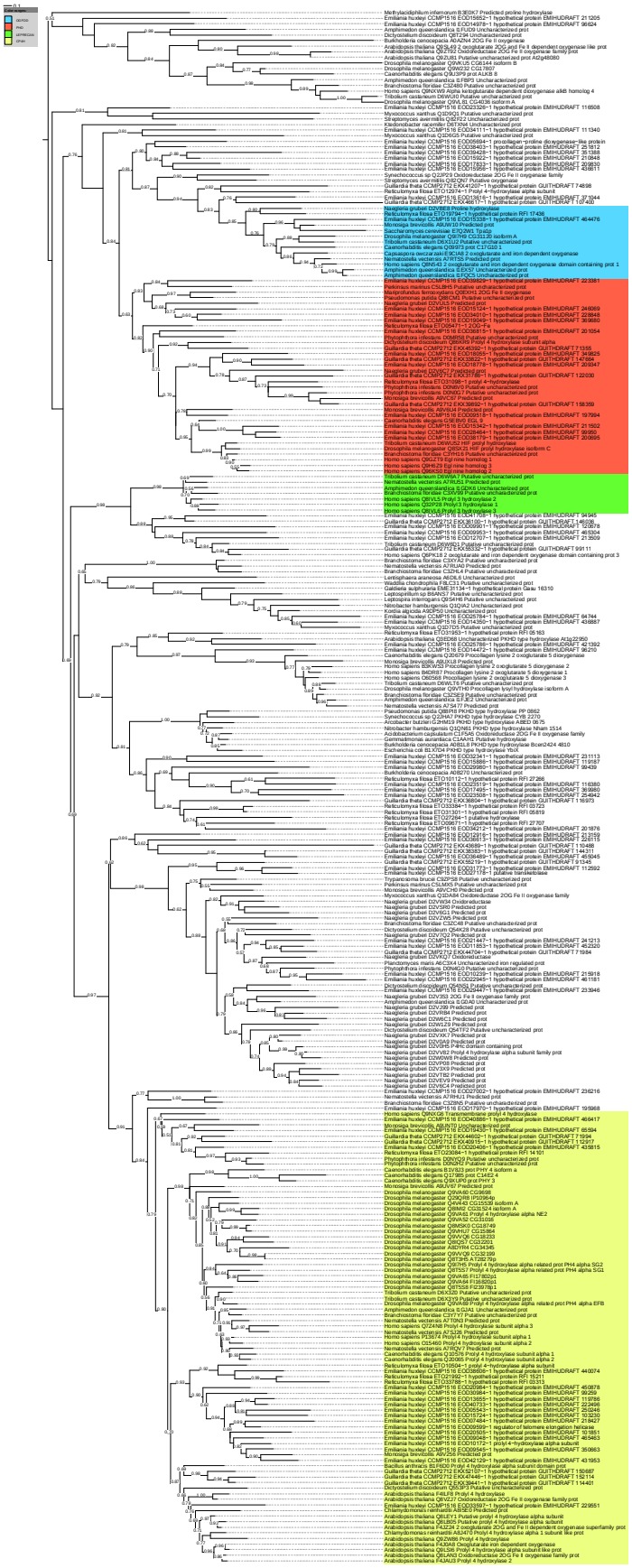

Fig. S8. Phylogenetic inference of putative prolyl-hydroxylases from selected taxa from major taxonomic groups in life. FastTree inference of 278 protein 2OG-FeII domain protein sequences under the WAG model of protein evolution reveals putative prolyl-hydroxylase clades corresponding to CP4H (yellow), PHD (red), Leprecan (green) and OGFOD1 (blue). Sequences were only considered in the OGFOD1 clade if they were also predicted to contain the Pfam domain Ofd1_CTDD (PF10637). SH support values of equal or greater than 50% are shown for each node. The scale bar represents 10% estimated sequence divergence. The tree is arbitrarily rooted in the alpha-ketoglutarate-dependent dioxygenase (AlkB) group (31, 32), a putative outgroup, to ease reading of the tree.